



Article

Molecular and Functional Relevance of $\text{Na}_V1.8$ -Induced Atrial Arrhythmogenic Triggers in a Human *SCN10A* Knock-Out Stem Cell Model

Nico Hartmann ^{1,2,†} , Maria Knierim ^{2,3,†}, Wiebke Maurer ^{1,2}, Nataliya Dybkova ^{1,2}, Gerd Hasenfuß ^{1,2}, Samuel Sossalla ^{1,2,4,‡} and Katrin Streckfuss-Bömeke ^{1,2,5,*}

¹ Clinic for Cardiology and Pneumology, University Medical Center, 37075 Göttingen, Germany; nico.hartmann@med.uni-goettingen.de (N.H.); wiebke.maurer@med.uni-goettingen.de (W.M.); ndybkov@med.uni-goettingen.de (N.D.); hasenfus@med.uni-goettingen.de (G.H.); samuel.sossalla@ukr.de (S.S.)

² DZHK (German Center for Cardiovascular Research), Partner Site Göttingen and Rhein Main, 61231 Bad Nauheim, Germany; maria.knierim@med.uni-goettingen.de

³ Clinic for Cardio-Thoracic and Vascular Surgery, University Medical Center, 37075 Göttingen, Germany

⁴ Departments of Cardiology at Kerckhoff Heart and Lung Center, Bad Nauheim and University of Giessen, 61231 Bad Nauheim, Germany

⁵ Institute of Pharmacology and Toxicology, University of Würzburg, 97078 Würzburg, Germany

* Correspondence: katrin.streckfuss-boemeke@uni-wuerzburg.de

† These authors contributed equally to this work.

‡ These authors contributed equally to this work.

Abstract: In heart failure and atrial fibrillation, a persistent Na^+ current (I_{NaL}) exerts detrimental effects on cellular electrophysiology and can induce arrhythmias. We have recently shown that $\text{Na}_V1.8$ contributes to arrhythmogenesis by inducing a I_{NaL} . Genome-wide association studies indicate that mutations in the *SCN10A* gene ($\text{Na}_V1.8$) are associated with increased risk for arrhythmias, Brugada syndrome, and sudden cardiac death. However, the mediation of these $\text{Na}_V1.8$ -related effects, whether through cardiac ganglia or cardiomyocytes, is still a subject of controversial discussion. We used CRISPR/Cas9 technology to generate homozygous atrial *SCN10A*-KO-iPSC-CMs. Ruptured-patch whole-cell patch-clamp was used to measure the I_{NaL} and action potential duration. Ca^{2+} measurements (Fluo 4-AM) were performed to analyze proarrhythmogenic diastolic SR Ca^{2+} leak. The I_{NaL} was significantly reduced in atrial *SCN10A* KO CMs as well as after specific pharmacological inhibition of $\text{Na}_V1.8$. No effects on atrial APD_{90} were detected in any groups. Both *SCN10A* KO and specific blockers of $\text{Na}_V1.8$ led to decreased Ca^{2+} spark frequency and a significant reduction of arrhythmogenic Ca^{2+} waves. Our experiments demonstrate that $\text{Na}_V1.8$ contributes to I_{NaL} formation in human atrial CMs and that $\text{Na}_V1.8$ inhibition modulates proarrhythmogenic triggers in human atrial CMs and therefore $\text{Na}_V1.8$ could be a new target for antiarrhythmic strategies.

Keywords: $\text{Na}_V1.8$; iPSC-cardiomyocytes; late Na^+ current (I_{NaL}); CRISPR Cas9



Citation: Hartmann, N.; Knierim, M.; Maurer, W.; Dybkova, N.; Hasenfuß, G.; Sossalla, S.; Streckfuss-Bömeke, K. Molecular and Functional Relevance of $\text{Na}_V1.8$ -Induced Atrial Arrhythmogenic Triggers in a Human *SCN10A* Knock-Out Stem Cell Model. *Int. J. Mol. Sci.* **2023**, *24*, 10189. <https://doi.org/10.3390/ijms241210189>

Academic Editors: Sorin Hostiuc and Buddhadeb Dawn

Received: 2 May 2023

Revised: 26 May 2023

Accepted: 13 June 2023

Published: 15 June 2023



Copyright: © 2023 by the authors. Licensee MDPI, Basel, Switzerland. This article is an open access article distributed under the terms and conditions of the Creative Commons Attribution (CC BY) license (<https://creativecommons.org/licenses/by/4.0/>).

1. Introduction

Voltage-gated sodium channels (Na_V) trigger the fast upstroke of the action potential (AP), making them important for the physiological conduction of electrical impulses in the heart. Under physiological conditions, Na_V channels (predominantly $\text{Na}_V1.5$) quickly become inactive after activation. However, in some cardiac pathologies such as ischemia and heart failure (HF), Na_V channels were described to remain persistently open or reopen, thus creating the late sodium current (I_{NaL}) as a persistent inward current [1–4]. It has been demonstrated that this pathologically enhanced I_{NaL} has detrimental effects on cellular electrophysiology and can induce arrhythmias [3,5–8]. Previous reports have been published on the existence of non-cardiac Na_V isoforms in the heart including $\text{Na}_V1.8$. $\text{Na}_V1.8$

is encoded by the *SCN10A* gene and described as a voltage-gated sodium channel like the predominant cardiac isoform $\text{Na}_V1.5$. $\text{Na}_V1.8$ has been shown to be predominantly expressed in neuronal tissues with mainly nociception functions and in human and rat spinal cord ganglia and cranial sensory ganglia [9–12]. Recent work has demonstrated that $\text{Na}_V1.8$ mRNA is expressed in murine and human myocardia [13,14]. In situ hybridization experiments displayed that $\text{Na}_V1.8$ has comparable cellular localizations to $\text{Na}_V1.5$ in murine cardiomyocytes [15]. Genome-wide association studies reported that variants in the *SCN10A* gene (coding for $\text{Na}_V1.8$) are associated with cardiac arrhythmias such as atrial fibrillation, sudden cardiac death [16,17], impaired conduction in the form of alterations in the PQ and QRS intervals, heart rate and increased arrhythmogenic risk [16], and with J-wave syndromes, specifically Brugada syndrome (BrS) and early repolarization syndrome (ERS) [18]. However, it remains controversial whether these $\text{Na}_V1.8$ -associated effects are mechanistically mediated by $\text{Na}_V1.8$ and, if so, if they occur in cardiac ganglia or cardiomyocytes (CMs). $\text{Na}_V1.8$ mRNA and protein were found to be significantly more abundant in human atrial myocardium compared to the ventricular myocardium. The expression levels of $\text{Na}_V1.8$ and $\text{Na}_V1.5$ did not show any differences between myocardial samples obtained from patients with atrial fibrillation and those with sinus rhythm [19–22]. Functional single-cell experiments of atrial and ventricular human and murine CMs demonstrated direct effects of pharmacological $\text{Na}_V1.8$ inhibition on the I_{NaL} and cellular arrhythmogenesis [19,22]. However, these studies were limited by utilizing respective ion channel blockers that could theoretically have unspecific effects. The currently available drugs, such as amiodarone, have limited efficacy, poor tolerability, and notable adverse side effects, including life-threatening ventricular arrhythmias. Clinical guidelines recommend amiodarone treatment for most patients with severe structural heart disease, especially heart failure (HF). However, chronic use of amiodarone can lead to severe extra-cardiac side effects and organ toxicity despite its relative effectiveness against arrhythmias. There is a demand for new and safer innovative compounds to address this issue. Therefore, we aimed to investigate the electrophysiological contribution of $\text{Na}_V1.8$ using CRISPR/Cas9-generated homozygous atrial *SCN10A* knock out (KO) induced-pluripotent stem cell CMs (iPSC-CMs). We ultimately describe the influence of the $\text{Na}_V1.8$ channel on the electrophysiological and molecular properties of human atrial CMs and further demonstrate that $\text{Na}_V1.8$ is a potential new target for atrial antiarrhythmic strategies.

2. Results

2.1. CRISPR/Cas9 Based Homozygous Knock-Out of *SCN10A* in Human Atrial iPSC-Cardiomyocytes

Homozygous *SCN10A*/ $\text{Na}_V1.8$ -deficient (*SCN10A* KO) human atrial iPSC-CMs were generated using CRISPR/Cas9 genome editing as previously described [22,23]. Full pluripotency, genome integrity and spontaneous differentiation capacity into all three germ layers were confirmed in *SCN10A* KO iPSCs [23]. Homozygous KO of the gene was confirmed by Sanger sequencing in two different *SCN10A*-KO iPSC cell lines [22,23] as well as in atrial differentiated *SCN10A* KO iPSC-CMs by showing premature stop codons on both alleles (A1: delC/insCAC → premature stop in Ex1 and A2: delCT → premature stop in Ex1) (Figure 1a). Successful differentiation of control and *SCN10A* KO iPSCs into atrial iPSC-CMs was demonstrated by immunostaining of atrial myosin light chain 2 isoform (MLC2a) (Figure 1b) and mRNA expression of the atrial marker PITX2 (Figure 1c).

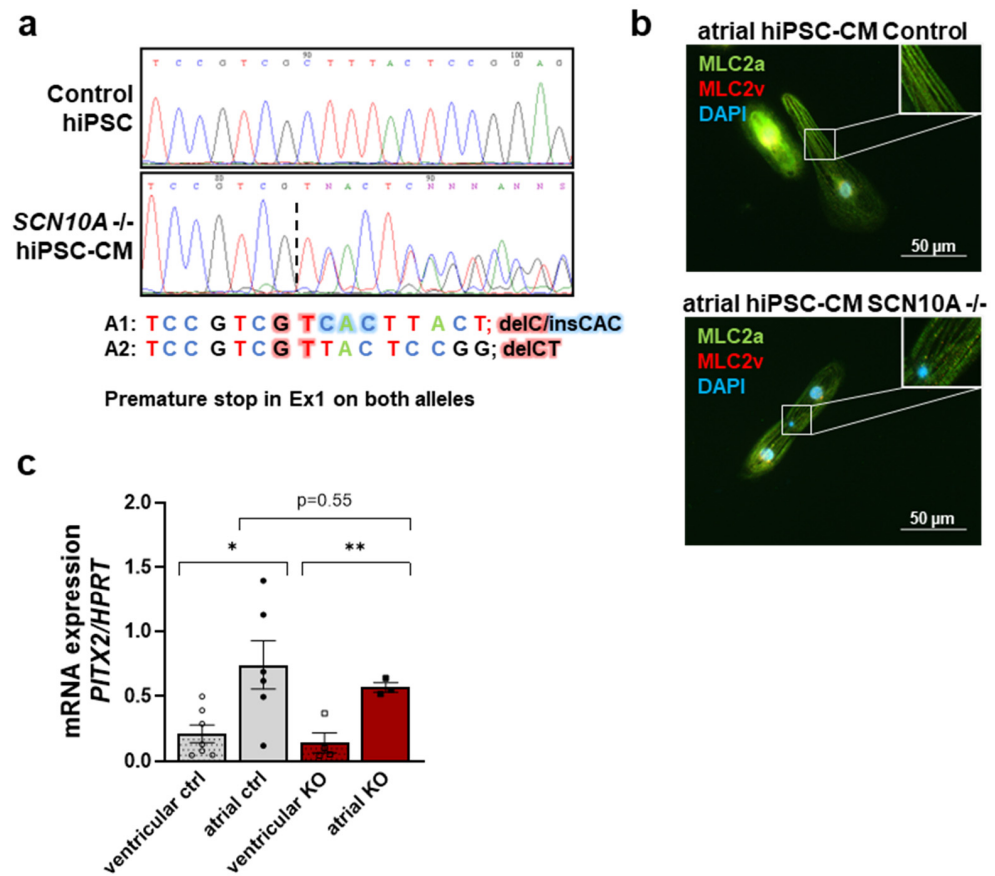


Figure 1. CRISPR/Cas9-based knock-out of *SCN10A*/*Nav*_v1.8 in atrial iPSC-CMs. (a) Sanger sequencing of control iPSCs and *SCN10A* iPSC-KO CMs demonstrating frameshifts in both alleles leading to a premature stop in exon 1 (A1: delC/insCAC and A2: delCT). (b) Atrial control and *SCN10A* KO iPSC-CMs were stained for MLC2a (green) and MLC2v (red) demonstrating atrial differentiation. Nuclei were stained with DAPI. (c) mRNA expression level of atrial marker PITX2 normalized to house-keeping gene HPRT in atrial control and *SCN10A* KO iPSC-CMs ($n = 6/3$ differentiations) compared to ventricular control and *SCN10A* KO iPSC-CMs ($n = 7/4$ differentiations). Student's t-test was applied for normally distributed data. *: $p < 0.05$; **: $p < 0.01$.

2.2. Influence of *Nav*_v1.8 on *I*_{NaL} in Human Atrial iPSC-Cardiomyocytes

We hypothesized that the KO of *SCN10A* in atrial iPSC-CMs would reduce the proarrhythmogenic *I*_{NaL}. Therefore, whole-cell voltage clamp experiments were performed to directly measure the *I*_{NaL} integral in human atrial *SCN10A* KO and control iPSC-CMs.

Since the amplitude of the *I*_{NaL} is relatively small in healthy hiPSC-CMs under physiological conditions [24], we used isoproterenol (Iso, 50 nmol/L) for slight beta-adrenergic stimulation in control and experimental groups during all functional experiments as described previously [20]. To further compare *SCN10A* KO with pharmacological inhibition of *Nav*_v1.8 and test for potential side effects of either KO or pharmacological intervention, we used the specific *Nav*_v1.8 blocker PF-01247324 (1 μ mol/L) [19,22]. Voltage-clamp experiments demonstrated that the *I*_{NaL} was significantly reduced by genetical KO of *Nav*_v1.8 as well as by pharmacological inhibition. The Iso-induced increase in the *I*_{NaL} in control iPSC-CMs ($-125.5 \pm 8.4 \text{ A} \cdot \text{ms} \cdot \text{F}^{-1}$) was significantly reduced in KO iPSC-CMs ($-34.4 \pm 4.8 \text{ A} \cdot \text{ms} \cdot \text{F}^{-1}$, $p < 0.0001$, Figure 2). Moreover, the *I*_{NaL} was reduced to the level of KO iPSC-CMs by application of the specific *Nav*_v1.8 inhibitor [PF-01247324, 1 μ mol/L, atrial control iPSC-CMs vs. PF-01247324 ($-44.9 \pm 3.8 \text{ A} \cdot \text{ms} \cdot \text{F}^{-1}$, $p < 0.001$, Figure 2)]. Notably, we observed no additional effects on the *I*_{NaL} in KO iPSC-CMs after application of PF-01247324.

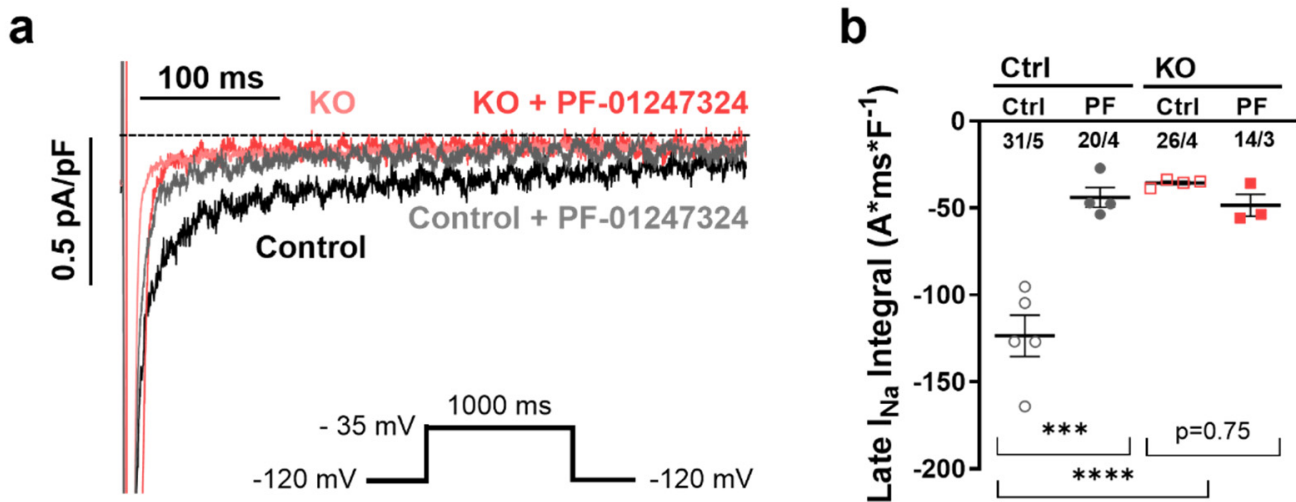


Figure 2. (a) Original traces of I_{NaL} in atrial control iPSC vs. *SCN10A* KO-iPSC cells according to the inserted protocol. (b) Mean values per differentiation \pm SEM of I_{NaL} (atrial control $n = 31$ cells/5 differentiations; atrial control + PF $n = 20$ cells/4 differentiations; *SCN10A* KO iPSC–CM control $n = 26$ cells/4 differentiations, *SCN10A* KO-iPSC-CMs+ PF $n = 14$ cells/3 differentiations). Mean values per differentiation were compared using one-way ANOVA with Sidak’s test for multiple comparisons to calculate p values (** = $p < 0.01$; *** = $p < 0.001$; **** = $p < 0.0001$).

2.3. Effects of $Na_v1.8$ on the Atrial Action Potential

To assess the potential influence of KO and pharmacological $Na_v1.8$ inhibition on the action potential characteristics in human atrial iPSC-CMs, we performed whole-cell current-clamp experiments. The data presented herein are representative of measurements conducted at a frequency of 1 Hz. No effects on atrial action potential duration at 90% repolarization (APD_{90}) were observed in KO iPSC-CMs as well as after the additional application of the specific $Na_v1.8$ blocker PF-01247324 (Figure 3a,b; control at 1.0 Hz, 243.0 ± 30.5 ms vs. control + PF 229.3 ± 19.0 ms, -5.8% ; KO control 204.4 ± 24.2 ms, -16% , vs. KO + PF 198.9 ± 30.1 ms, -3%). Furthermore, no discernible impacts were observed on the duration of atrial action potential at 20% repolarization (APD_{20}), action potential duration at 50% repolarization (APD_{50}), and action potential duration at 70% repolarization (APD_{70}). The available data, including Table S1 and Figure S1, were included in the Supplemental Materials. To rule out potential side effects of KO or pharmacological inhibition of $Na_v1.8$, we compared the resting membrane potential and action potential amplitude in all groups. No significant effects of KO or pharmacological inhibition of $Na_v1.8$ on either AP amplitude (APA, Figure 3c, 113.7 ± 4.4 ms vs. control + PF 118.7 ± 3.4 ms, KO control 105.7 ± 5.1 ms, KO + PF 102.1 ± 4.2 ms), resting membrane potential (RMP, Figure 3d; -76.0 ± 6.2 ms vs. control + PF -72.2 ± 5.7 ms; KO control -66.7 ± 2.6 ms vs. KO + PF -67.3 ± 3.9 ms), or upstroke velocity (V_{max} , Figure 3e; 106.2 ± 11.2 vs. control + PF 127.5 ± 11.9 mV/ms; KO control 92.7 ± 13.8 vs. KO + PF 82.8 ± 12.4 mV/ms) could be observed.

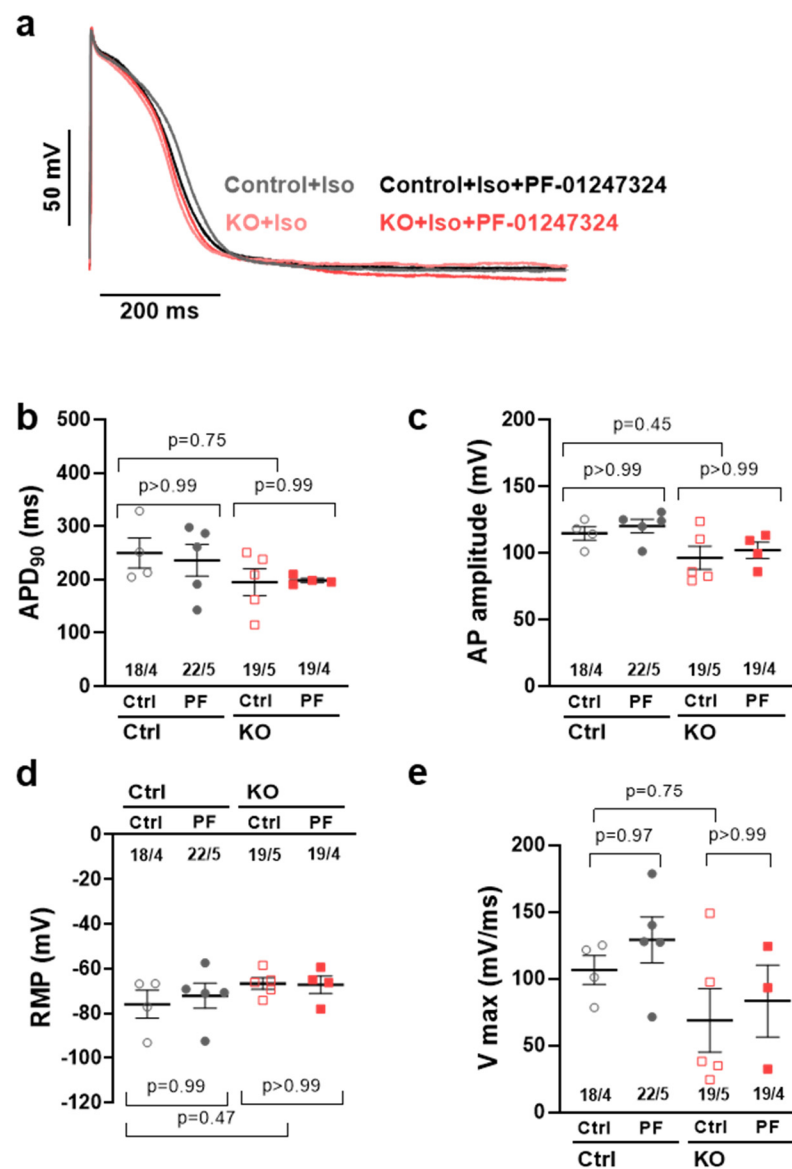


Figure 3. (a) Original traces of APD₉₀ in atrial control iPSC-CMs vs *SCN10A* KO-iPSC-CMs at 1 Hz. (b) Mean (nested) \pm SEM of APD₉₀ (atrial control $n = 18$ cells/4 differentiations; atrial control + PF $n = 22$ cells/5 differentiations; *SCN10A* KO control $n = 19$ cells/5 differentiations; *SCN10A* KO + PF $n = 19$ cells/4 differentiations); statistics calculated using nested oneway ANOVA. (c) Mean \pm SEM of amplitude (atrial control $n = 18$ cells/4 differentiations; atrial control + PF $n = 22$ cells/5 differentiations; *SCN10A* KO control $n = 19$ cells/5 differentiations; *SCN10A* KO + PF $n = 19$ cells/4 differentiations). (d) Mean \pm SEM of RMP (atrial control $n = 18$ cells/4 differentiations; atrial control + PF $n = 22$ cells/5 differentiations; *SCN10A* KO control $n = 19$ cells/5 differentiations; *SCN10A* KO + PF $n = 19$ cells/4 differentiations); statistics calculated using nested one-way ANOVA. (e) Mean \pm SEM of V_{max} (atrial control $n = 18$ cells/4 differentiations; atrial control + PF $n = 22$ cells/5 differentiations; *SCN10A* KO control $n = 19$ cells/5 differentiations; *SCN10A* KO + PF $n = 19$ cells/4 differentiations).

2.4. Effects of Na_v1.8 on Atrial Sarcoplasmic Reticulum Ca²⁺ Leak and Arrhythmogenesis

As we previously demonstrated, Na_v1.8 exerts its arrhythmogenic potential in the atria via enhancement of the I_{NaL} [19]. To investigate the functional cellular effects of the Na_v1.8-dependent I_{NaL} on Ca²⁺ homeostasis and cellular arrhythmogenesis in atrial iPSC-CMs, we recorded line scans in confocal microscopy experiments using Fluo 4-AM in human atrial *SCN10A* KO and control iPSC-CMs. Diastolic confocal line scans (Fluo

4-AM) showed that KO of *SCN10A* in atrial iPSC-CMs massively decreased the frequency of spontaneous arrhythmogenic Ca^{2+} sparks compared to the respective control cells (KO: 3.25 ± 0.23 sparks/100 $\mu\text{m}^2/\text{s}$ vs. control: 6.34 ± 0.43 , $p = 0.0142$). Similarly, pharmacological inhibition of $\text{Na}_V1.8$ by PF-01247324 led to a significant reduction of diastolic Ca^{2+} sparks in atrial control iPSC CMs (control + PF-01247324: 3.96 ± 0.21 , $p = 0.0469$), while having no further effect on *SCN10A* KO cells (KO + PF-01247324: 3.47 ± 0.34 , $p = 0.9998$) (Figure 4a,b). Furthermore, we investigated the incidence of spontaneous diastolic Ca^{2+} waves as major arrhythmogenic events. The proportion of cells exhibiting diastolic Ca^{2+} waves was significantly reduced from 24.7% in atrial control -iPSC-CMs to 5.5% in the *SCN10A* KO group. After pharmacological inhibition of $\text{Na}_V1.8$, we observed a comparable reduction of cells displaying Ca^{2+} waves compared to control (9.0%). There was no significant additional effect of $\text{Na}_V1.8$ inhibition in *SCN10A* KO cells (8.7%) (Figure 4c,d).

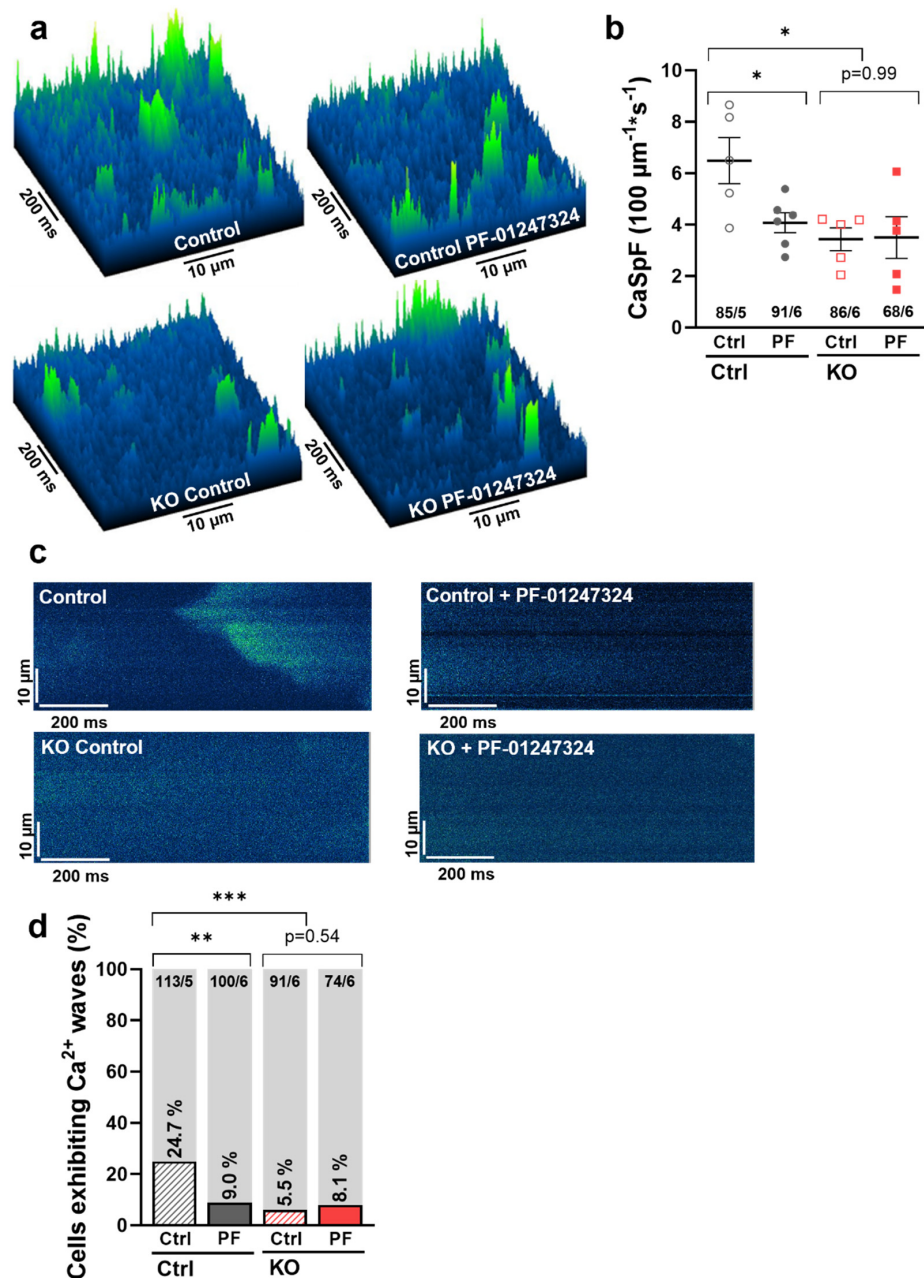


Figure 4. Contribution of $\text{Na}_V1.8$ to spontaneous diastolic sarcoplasmic reticulum Ca^{2+} release in atrial iPSC-CMs. (a) Representative surface plots showing spontaneous diastolic Ca^{2+} sparks (green)

in atrial iPSC-CMs. (b) Mean values of Ca^{2+} spark frequency (CaSpF) normalized to scan width and duration. Numbers indicate total cell count of control CMs (atrial control, $n = 85$ cells/5 differentiations), control cells treated with $\text{Na}_V1.8$ inhibitor PF01247324 (atrial control + PF-01247324, $n = 91/6$), and atrial CMs with KO of $\text{Na}_V1.8$ after control treatment and treatment with PF-01247324 ($n = 86/6$ vs. $68/6$). Symbols indicate the mean values of different differentiation experiments. (c) Original representative line scans of atrial iPSC-CMs illustrating a spontaneous proarrhythmic diastolic Ca^{2+} wave (green). (d) Percentage of cells exhibiting diastolic Ca^{2+} waves in relation to cells without Ca^{2+} waves (grey bars) in atrial control CMs (24.7%, $n = 28$ of 113 cells from 5 differentiations) compared to atrial control CMs + PF-01247324 (9%, $n = 9/100$ cells/6 diff.) and to atrial SCN10A KO CMs with inhibition of $\text{Na}_V1.8$ by PF-01247324 (8.1%, $n = 6/74$ cells/6 diff.) or without (5.5%, $n = 5/91$ cells/6 diff.). Values are presented as mean \pm SEM or absolute numbers. Mean values per differentiation were compared using one-way ANOVA with Sidak's test for multiple comparisons to calculate p values. Proportions were compared using Fisher's exact test (* = $p < 0.05$, ** = $p < 0.01$; *** = $p < 0.001$).

2.5. Influence of SCN10A KO on Intracellular Ca^{2+} Transients

Since KO of SCN10A was shown to reduce the arrhythmogenic potential of the increased I_{NaL} in atrial human iPSC-CMs by reduction of spontaneous SR Ca^{2+} release events, we further sought to rule out any potential adverse effects on cellular Ca^{2+} handling.

We therefore performed epifluorescence microscopy (Fura 2-AM) in atrial iPSC-CMs with and without KO of SCN10A and/or pharmacological inhibition of $\text{Na}_V1.8$. SCN10A KO did not show any significant effects on Ca^{2+} transient amplitude, diastolic Ca^{2+} levels, time to peak, or relaxation time (RT 80%), demonstrating intact Ca^{2+} handling in both KO and WT cells. Of note, specific inhibition of $\text{Na}_V1.8$ by PF-01247324 also did not exert any additional effects on Ca^{2+} transient parameters in either control or KO atrial iPSC-CMs (Figure 5).

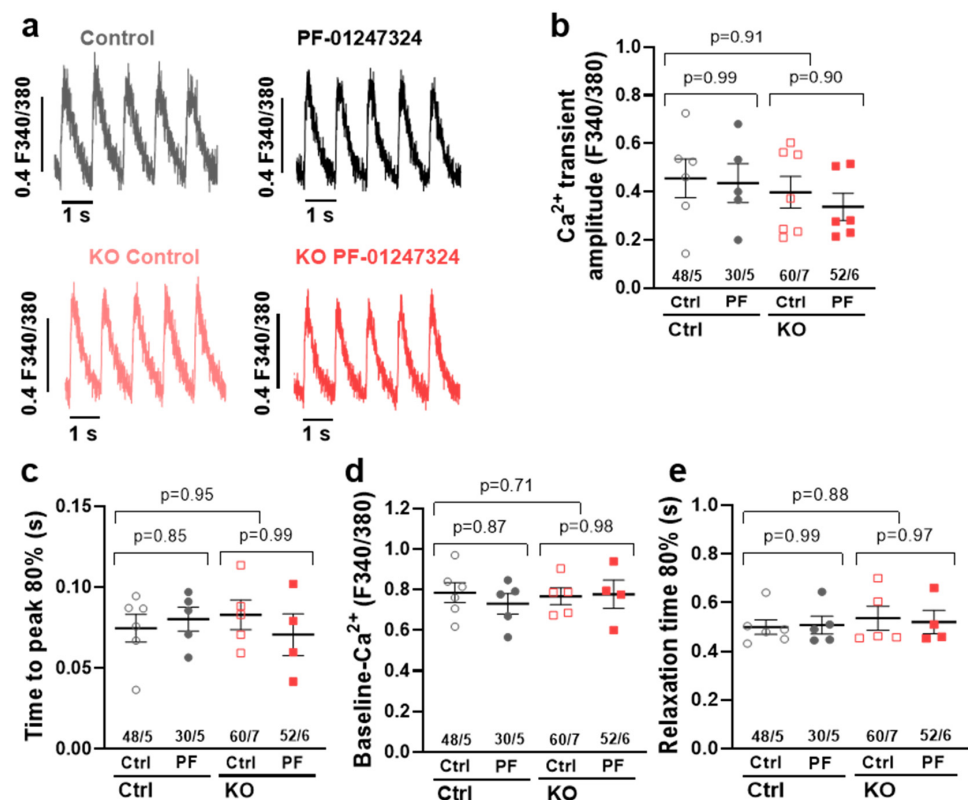


Figure 5. (a) Representative original recordings of stimulated systolic Ca^{2+} transients (epifluorescence microscopy, Fura 2-AM, 1 Hz) of human atrial SCN10A or control iPSC-CMs and after additional $\text{Na}_V1.8$

inhibition by PF-01247324. Mean values \pm SEM of (b) systolic Ca^{2+} transient amplitude, (c) time to peak 80%, (d) diastolic Ca^{2+} level, and (e) relaxation time 80% in control CMs ($n = 48$ cells/5 differentiations), *SCN10A* KO CMs ($n = 60/7$), and each after treatment with PF-01247324 (control + PF-01247324 $n = 30/5$, KO + PF-01247324 $n = 52/6$). Values are presented as mean \pm SEM. Mean values per differentiation were compared using one-way ANOVA with Sidak's test for multiple comparisons to calculate p values.

2.6. The Expression of Key Proteins of Excitation–Contraction Coupling Is Not Altered by a *SCN10A* KO

Since we demonstrated a reduction in the arrhythmogenic potential in atrial human *SCN10A* KO iPSC-CMs, we wanted to analyze the potential underlying effects on a molecular level. Therefore, we investigated the expression of key proteins of excitation–contraction coupling (voltage-gated sodium channel isoform $\text{Na}_V1.5$; L-type Ca^{2+} channel $\text{Ca}_V1.2$; cardiac ryanodine receptor 2, RyR_2) using Western blot experiments.

In atrial control iPSC-CMs, we found a lower expression of $\text{Na}_V1.5$ compared to *SCN10A* KO iPSC-CMs, but it did not reach statistical significance (Figure 6a,d). Furthermore, RyR_2 and $\text{Ca}_V1.2$ were not regulated in atrial *SCN10A* KO iPSC-CMs compared to control atrial iPSC-CMs according to the Western blot results (Figure 6b,c,e,f). Thus, *SCN10A* KO seems to exert no significant side effects on the expression of the other main proteins relevant to excitation–contraction coupling in atrial iPSC-CMs compared with their respective control cells.

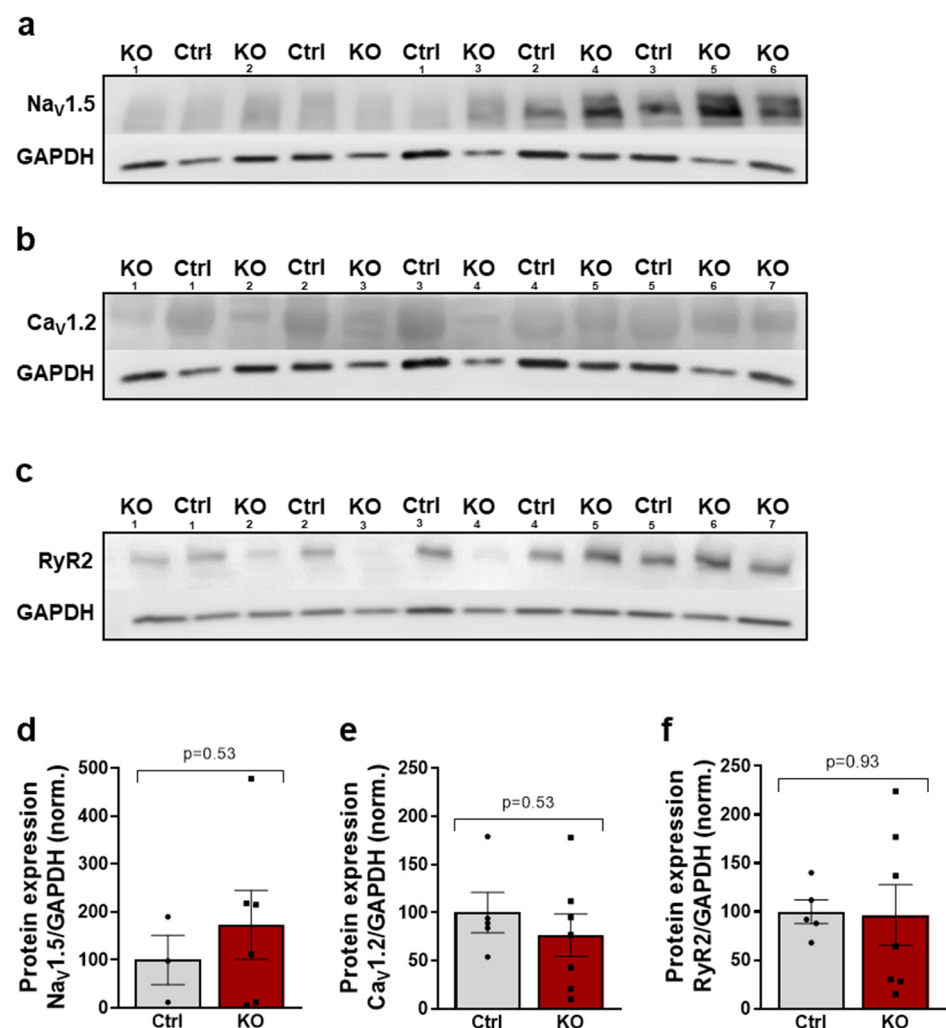


Figure 6. Original Western blots of $\text{Na}_V1.5$ (a), $\text{Ca}_V1.2$ (b), and RyR_2 (c) in atrial control and *SCN10A*

KO iPSC-CMs. Normalized values of $\text{Na}_V1.5$ (d) ($n = 3$ control/6 KO differentiations), $\text{Ca}_V1.2$ (e) ($n = 5/7$ differentiations), and RyR2 (f) ($n = 5/7$ differentiations) in atrial control and *SCN10A* KO iPSC-CMs normalized to GAPDH ($n = 5/7$ differentiations). Student's t-test was used for statistical analysis.

3. Discussion

Atrial fibrillation (AF) is the most prevalent clinically significant arrhythmia. It represents a major risk factor for embolic stroke and exacerbation of heart failure (HF), consequently contributing to heightened morbidity and mortality rates [25]. The current prevalence of atrial fibrillation (AF) in adults ranges between 2% and 4%, with an anticipated 2.3-fold increase due to the extended longevity of the general population. For patients with atrial fibrillation (AF), first-line therapies for rhythm control include anti-arrhythmic drugs and/or left atrial pulmonary vein ablation [25]. However, pharmacological rhythm control is notably restricted in patients with underlying structural heart disease. The currently available drugs for these patients have limitations, poor tolerability, and adverse side effects [26]. Therefore, there is a demand for new and safer innovative compounds to address the treatment of AF in patients with structural heart disease. Sodium currents are effective therapeutic targets for the treatment of AF. In this context, the I_{NaL} has been increasingly identified as a potential target to inhibit cellular arrhythmogenic triggers in AF and the first hopeful results have been shown in clinical trials [26–30].

However, the mechanism of I_{NaL} regulation with respect to cellular arrhythmogenic triggers is not yet well understood. Besides $\text{Na}_V1.5$, other Na_V isoforms have been reported to be present in the heart. We have shown that the expression of the Na^+ channel $\text{Na}_V1.8$ in left ventricular CMs is upregulated in human HF myocardium [20], and that $\text{Na}_V1.8$ contributes to arrhythmogenesis by inducing the I_{NaL} [19,20,22,31]. Variants in the *SCN10A* gene ($\text{Na}_V1.8$) were shown to be associated with cardiac arrhythmias such as atrial fibrillation and sudden cardiac death [32]. Whether these $\text{Na}_V1.8$ -related effects are mediated by cardiac ganglia or cardiomyocytes is still under debate. In the present study, we used human atrial *SCN10A* KO iPSC-CMs and demonstrated that $\text{Na}_V1.8$ is responsible for the generation of the I_{NaL} . Both inhibition and KO of $\text{Na}_V1.8$ potently suppressed the I_{NaL} and diastolic SR-Ca^{2+} leak as proarrhythmogenic triggers in atrial CMs. These findings suggest that targeting $\text{Na}_V1.8$ constitutes a novel therapeutic antiarrhythmic strategy for the treatment of atrial rhythm disorders.

3.1. $\text{Na}_V1.8$ and Atrial I_{NaL}

Under pathological conditions, the enhanced persistent Na^+ influx, known as enhanced I_{NaL} , has been demonstrated to play an important role throughout the action potential [33]. The prolongation of the action potential duration caused by an I_{NaL} increases the likelihood of early afterdepolarizations (EADs), which serve as triggers for the occurrence of arrhythmias. The specific Na_V isoforms involved in the generation of an I_{NaL} , particularly in clinically relevant conditions like atrial fibrillation (AF) and heart failure (HF), remain unclear. This information is of translational relevance because selectively targeting the inhibition of the I_{NaL} would be a desirable antiarrhythmic approach.

Genome-wide association studies have identified *SCN10A* as a regulator of cardiac conduction. By employing various methodologies in both human and mouse cardiomyocytes, we have demonstrated the significance of $\text{Na}_V1.8$ in the generation of the late sodium current (I_{NaL}). We found that $\text{Na}_V1.8$ is upregulated under conditions of HF and cardiac hypertrophy [20,22,31]. Recent studies have provided evidence for the involvement of $\text{Na}_V1.8$ in atrial cellular electrophysiology and have successfully linked *SCN10A* variants to AF [32,34]. However, some of the preliminary studies are limited by the use of appropriate ion channel blockers, which theoretically could have nonspecific effects.

Therefore, in the present study we used homozygous atrial *SCN10A*-KO iPSC-CMs to show that the $\text{Na}_V1.8$ -associated effects are mechanistically mediated by $\text{Na}_V1.8$. Since under healthy conditions the I_{NaL} is very low, we applied isoproterenol in order to enhance the I_{NaL} for a better comparison between the control and KO iPSC CMs. Casini et al. did not detect any $\text{Na}_V1.8$ -based I_{NaL} in non-diseased human atrial and rabbit ventricular CMs without beta-adrenergic stimulation [24]. Most importantly, the incidence of an enhanced I_{NaL} depends on pharmacological (beta-adrenergic activation) or pathological stimulation and explain the absence of $\text{Na}_V1.8$ effects in this study. Here, we show that $\text{Na}_V1.8$ contributes to an enhanced I_{NaL} in atrial control iPSC-CMs by reducing the I_{NaL} by simultaneous treatment with isoproterenol and PF-01247324. Moreover, the specific blocker PF-01247324, when used to inhibit $\text{Na}_V1.8$, did not induce any additional effects on the I_{NaL} in $\text{Na}_V1.8$ KO atrial cells compared to untreated $\text{Na}_V1.8$ KO atrial cells. This finding highlights the specificity of the drug in targeting $\text{Na}_V1.8$ [35]. Pabel et al. demonstrated that both pharmacological inhibition and genetic ablation of $\text{Na}_V1.8$ resulted in a reduction of the late sodium current (I_{NaL}) in human and murine atrial CMs [19]. In line with this, patch-clamp recordings of isolated human atrial CMs obtained from patients in sinus rhythm revealed that following mild beta-adrenergic stimulation with isoproterenol, the inhibition of $\text{Na}_V1.8$ using PF-01247324 and A-803467 led to a significant reduction in the late sodium current (I_{NaL}) [19]. Isolated atrial CMs from *SCN10A*^{-/-} mice revealed a significantly lower I_{NaL} compared to WT while pharmacological inhibition by PF-01247324 exerted no additional effect on the I_{NaL} in *SCN10A*^{-/-} mice [19]. Therefore, the results of the present study are in line with previous findings in atrial human and mice atrial KO [19] and ventricular KO mice and human iPSC-CMs and isolated CMs [22,36]. Moreover, the impact of *SCN10A* variants associated with AF on the modulation of the I_{NaL} was demonstrated through transfection experiments in ND7/23 cells. This additional evidence further strengthens the notion that $\text{Na}_V1.8$ plays a significant role in the development of I_{NaL} -related arrhythmias [37].

3.2. $\text{Na}_V1.8$ and Atrial Action Potential Duration

Previous studies have provided evidence that the I_{NaL} plays a significant role in determining the APD in both atrial and ventricular CMs [2,3,8,27,29]. Having demonstrated the upregulation of $\text{Na}_V1.8$ expression in human AF and HF, we proceeded to investigate the impact of $\text{Na}_V1.8$ -induced I_{NaL} on various action potential parameters. We also used isoproterenol to enhance the I_{NaL} . In line with previous data from our group in atrial human and mice CMs [19], the present study showed that in atrial control or *SCN10A* KO iPSC CMs, $\text{Na}_V1.8$ has negligible effects on the atrial action potential parameters. In AF, the APD becomes shorter and a further shortening of APD may lead to shorter refractory periods, thereby further facilitating reentry. Therefore, negligible effects on APD point towards a positive therapeutic profile of targeting $\text{Na}_V1.8$ in AF. Since dv/dt is a surrogate for the fast Na^+ influx and peak Na^+ current, these data show that there is no involvement of $\text{Na}_V1.8$ in the peak Na^+ current in atrial iPSC CMs. A negligible effect of $\text{Na}_V1.8$ inhibition on cardiac conduction peak Na^+ current blockade would be desirable in order to treat patients with structural heart disease and AF.

3.3. $\text{Na}_V1.8$ and Atrial Ca^{2+} Handling

In our previous studies, we demonstrated that the I_{NaL} -mediated Na^+ influx has the ability to induce Ca^{2+} influx through reverse-mode NCX, resulting in elevated cytosolic $[\text{Ca}^{2+}]$ levels and an increased occurrence of Ca^{2+} sparks in the human atrium [21,28]. Furthermore, the inhibition of the I_{NaL} through specific targeting of $\text{Na}_V1.8$ has the capability to reduce the reverse mode NCX, thereby also mitigating diastolic proarrhythmogenic SR- Ca^{2+} leak [20,21,31]. The relationship between enhanced I_{NaL} and an increased risk of arrhythmias is indeed complex. This complexity arises from the fact that the increased leak of Ca^{2+} from the SR can induce a transient inward current, which, in turn, leads to

arrhythmogenic delayed afterdepolarizations. Additionally, it can also result in significant spontaneous proarrhythmic Ca^{2+} release from the SR [8,28].

In the present study, we show a reduction in spontaneous SR Ca^{2+} spark frequency as well as a decreased frequency of spontaneous Ca^{2+} waves in human atrial *SCN10A* KO CMs and in control CMs after pharmacological inhibition. As Ca^{2+} waves represent a major proarrhythmic trigger, we hereby establish the principle of $\text{Na}_V1.8$ -induced I_{NaL} and its triggering role in cellular arrhythmogenesis that is independent of neuronal influence in isolated human atrial CMs. Interestingly, we found no effects on intracellular Ca^{2+} transients in either *SCN10A* KO or following $\text{Na}_V1.8$ inhibition in control CMs. Thus, we propose that the intracellular Ca^{2+} handling and likely contractile function of CMs remain mostly unaffected by $\text{Na}_V1.8$. In summary, our results and current evidence indicate that the discussed $\text{Na}_V1.8$ -induced I_{NaL} mainly influences arrhythmogenesis on a subcellular level while leaving cellular Ca^{2+} release and contractile function unaffected.

3.4. Clinical Relevance

The currently available anti-arrhythmic drugs, particularly for patients with structural heart disease, are limited in their effectiveness. Drugs like flecainide or amiodarone, which are commonly used, demonstrate suboptimal efficacy and are associated with significant adverse side effects, including life-threatening ventricular arrhythmias and organ toxicity. Therefore, new, safer, and more precise compounds for the treatment of atrial arrhythmias are highly desirable. $\text{Na}_V1.8$ was detected in atria, and human hypertrophied and failing ventricles [19,22,31]. The results of the present study demonstrate that either genetic ablation of $\text{Na}_V1.8$ using *SCN10A* KO iPSC-CMs or pharmacological inhibition can reverse cellular proarrhythmic effects in the atria. Both inhibition and KO of $\text{Na}_V1.8$ potently suppressed proarrhythmogenic triggers (e.g., I_{NaL} and diastolic SR- Ca^{2+} leak) while leaving the peak Na^+ current unaffected. These findings suggest targeting $\text{Na}_V1.8$ -dependent I_{NaL} constitutes a novel therapeutic anti-arrhythmic strategy for the treatment of atrial rhythm disorders.

4. Materials and Methods

4.1. Generation of Homozygous Knockout iPSCs Using CRISPR/Cas9 and Directed Differentiation into Atrial iPSC-Cardiomyocytes

All procedures conducted in this study adhered to the principles outlined in the Declaration of Helsinki and received approval from the local ethics committee of the University Medicine of Göttingen (Az-10/9/15). Informed consent was signed by all tissue donors. A homozygous *SCN10A* KO iPSC line was generated from a control iPSC line by CRISPR/Cas9 genome editing as described in detail in previous studies [22,23]. The generated *SCN10A* KO iPSCs were differentiated into functionally beating, atrial iPSC-derived cardiomyocytes as described in [38].

In order to achieve directed atrial cardiac differentiation of the induced pluripotent stem cells (iPSCs), manipulation of the Wnt signaling pathway was employed, as previously described [38]. The cells were cultured for 60 days and then passaged onto glass-bottom Fluoro Dishes (WPI, 30 K/dish) by subjecting them to trypsinization at 37 °C for 3 min. The cells were allowed to settle for 7 days prior to further measurements, with medium changes performed every 2 days. iPSC-derived cardiac myocytes (iPSC-CMs) were analyzed 8–10 weeks after the initiation of differentiation, unless otherwise specified. The purity of the iPSC-CMs was determined by flow analysis, with a focus on cardiac troponin T positivity (>90% cardiac TNT+), as well as through qPCR and immunofluorescence analysis of atrial-specific markers (PITX2, MLC2a). Four to five differentiation experiments were performed to generate atrial iPSC-CMs from two $\text{Na}_V1.8$ knockout lines and their corresponding healthy isogenic control line.

4.2. Pharmacological Intervention

For selective inhibition of $\text{Na}_V1.8$ -induced sodium currents, a specific $\text{Na}_V1.8$ blocker PF-01247324 (1 $\mu\text{mol/L}$, Sigma-Aldrich, Taufkirchen, Germany) was used. Cellular electrophysiological measurements were performed under slight beta-adrenergic stimulation (isoproterenol (Iso), 50 nmol/L, Sigma-Aldrich, Taufkirchen, Germany) [20]. Prior to the start of experiments, the CMs were incubated for 15 min with both substances or isoproterenol alone as a control.

4.3. Patch-Clamp Experiments

The patch-clamp experiments were performed as previously described [19,22]. Briefly, 35,000 atrial iPSC-CMs were plated on glass-bottom Fluoro Dishes and incubated with either isoproterenol (50 nmol/L, Sigma-Aldrich, Taufkirchen, Germany) or isoproterenol + PF01247324 (1 $\mu\text{mol/L}$, Sigma-Aldrich, Taufkirchen, Germany) for 15 min before starting the measurements. The experiments were conducted at room temperature.

Action potential recordings were performed using the whole-cell patch-clamp technique. To elicit action potentials, square current pulses with amplitudes of 0.5–1 nA and durations of 1–5 ms were applied. The stimulation frequency was increased gradually from 0.5 to 2 Hz.

The late sodium current (I_{NaL}) was measured using the ruptured-patch whole-cell patch-clamp technique. The pipette used had a resistance ranging from 2 to 3 mega-ohms ($\text{M}\Omega$). I_{NaL} recordings were performed exclusively in CMs where a seal with a resistance of over 1 giga-ohm ($\text{G}\Omega$) was achieved, and the access resistance remained below 7 $\text{M}\Omega$. After a stabilization period of 3 min, the iPSC-derived CMs were held at a holding potential of -120 mV and then depolarized to -35 mV for 1000 ms with 10 pulses and a basic cycle length of 2 s. The I_{NaL} was quantified as the integral current amplitude between 100 and 500 ms and was normalized to the membrane capacitance.

4.4. Confocal Ca^{2+} Imaging

A total of 35,000 atrial iPSC-CMs plated on glass-bottom FluoroDishes were incubated with the Ca^{2+} indicator Fluo 4-AM (10 $\mu\text{mol/L}$, Invitrogen, Darmstadt, Germany) for 15 min at RT for de-esterification of the dye. The solution was substituted with Tyrode's solution (as described in [19]) and the respective pharmacological agents and left to incubate for 15 min. Confocal line scans were obtained with a laser scanning confocal microscope (LSM 5 Pascal, Zeiss, Jena, Germany). Scans were conducted after continuous electrical field stimulation at 1 Hz during pausing of stimulation. Ca^{2+} release events were analyzed using the SparkMaster plugin for ImageJ. The mean Ca^{2+} spark frequency was calculated from the number of sparks normalized to scan width, duration, and scan rate (100 $\mu\text{m/s}$). Cells exhibiting major Ca^{2+} release events (Ca^{2+} wavelets or waves) were excluded from the calculation of Ca^{2+} spark frequency and separately classified as proarrhythmic cells as a proportion of all cells.

4.5. Epifluorescence Microscopy for Ca^{2+} Transient Measurements

A total of 35,000 atrial CMs were dissociated and plated as described above and loaded with the radiometric Ca^{2+} indicator Fura 2-AM (5 $\mu\text{mol/L}$, Invitrogen) for 15 min at RT. Subsequently, the cells were washed with Tyrode's solution for de-esterification and incubated with pharmacological agents as described above. The measurements were performed using a fluorescence detection system (IonOptix, Amsterdam, Netherlands) connected to an inverted microscope with oil immersion lens (40 \times). Cardiomyocytes were subjected to electrical field stimulation at 1 Hz for the duration of the experiment to ensure steady intracellular Ca^{2+} concentrations. Recording of Ca^{2+} transients for analysis was performed at 1 Hz at steady state. For each cell, the stimulation was paused for 30 s to detect spontaneous Ca^{2+} release events and evaluate the spontaneous beating frequency of the iPSC-CMs. Ca^{2+} transients were analyzed using the software IonWizard (IonOptix).

4.6. Statistical Analysis

The data are reported as mean \pm SEM, unless otherwise stated. Analysis was carried out with Prism 9 software (Graphpad, San Diego, CA, USA). For comparisons of two groups, unpaired Student's *t* test was used in the case of parametric distribution of the data. Three or more groups including more than one differentiation experiment were compared using nested one-way ANOVA. The results were corrected for multiple comparisons by Sidak's correction. Fisher's exact test was used to statistically compare proportions. *p* values are two-sided and considered statistically significant if *p* < 0.05.

5. Conclusions

In conclusion, we showed that the neuronal sodium channel Na_V1.8, which contributes to the I_{NaL} in the heart, is down-regulated in atrial *SCN10A*-KO iPSC-CMs and, importantly, contributes to I_{NaL} formation in human atrial CMs. Na_V1.8 KO or the inhibition of Na_V1.8 modulates proarrhythmic triggers such as I_{NaL} and diastolic SR-Ca²⁺ leak in human atrial CMs. Therefore, Na_V1.8 might represent a novel treatment target for antiarrhythmic strategies.

Supplementary Materials: The following supporting information can be downloaded at: <https://www.mdpi.com/article/10.3390/ijms241210189/s1>.

Author Contributions: Conceptualization, N.H. and S.S.; Data curation, N.H. and M.K.; Formal analysis, N.H., M.K. and N.D.; Funding acquisition, N.H. and G.H.; Investigation, N.H. and M.K.; Methodology, N.H., M.K., W.M., N.D., S.S. and K.S.-B.; Project administration, S.S.; Resources, N.D., G.H. and S.S.; Software, M.K. and N.D.; Supervision, G.H. and K.S.-B.; Validation, N.H., M.K. and S.S.; Visualization, N.H., M.K., W.M. and N.D.; Writing—original draft preparation, N.H. and M.K. All authors have read and agreed to the published version of the manuscript.

Funding: This work was supported by the Else-Kröner-Fresenius Foundation to N.H. (2020_EKEA.56); German Heart Foundation/German Foundation of Heart Research (to S.S.) and SFB 1002 (to G.H.); and grants from the Deutsche Forschungsgemeinschaft (DFG) through the International Research Training Group Award (IRTG) 1816 (to K.S.-B.; W.M. is a fellow under IRTG 1816), and to K.S.-B. and S.S. (471241922)).

Institutional Review Board Statement: The study was conducted in accordance with the Declaration of Helsinki, and approved by the local Ethics Committee of the University Medical Center Göttingen (Az-10/9/15). Informed consent was obtained from all subjects involved in the study.

Informed Consent Statement: Not applicable.

Data Availability Statement: Not applicable.

Acknowledgments: We thank Yvonne Metz and Johanna Heine for their excellent technical assistance.

Conflicts of Interest: N.H. and M.K. declare no conflicts of interest. K.S.-B. has no competing interest directly related to this work, but has grants from Novartis. S.S. received speaker's/consultancy honoraria from Boehringer Ingelheim, AstraZeneca, Berlin-Chemie, Novartis, and Lilly.

References

1. Valdivia, C.R.; Chu, W.W.; Pu, J.; Foell, J.D.; Haworth, R.A.; Wolff, M.R.; Kamp, T.J.; Makielski, J.C. Increased late sodium current in myocytes from a canine heart failure model and from failing human heart. *J. Mol. Cell. Cardiol.* **2005**, *38*, 475–483. [[CrossRef](#)] [[PubMed](#)]
2. Maltsev, V.A.; Silverman, N.; Sabbah, H.N.; Undrovinas, A.I. Chronic heart failure slows late sodium current in human and canine ventricular myocytes: Implications for repolarization variability. *Eur. J. Heart Fail.* **2007**, *9*, 219–227. [[CrossRef](#)] [[PubMed](#)]
3. Song, Y.; Shryock, J.C.; Belardinelli, L. An increase of late sodium current induces delayed afterdepolarizations and sustained triggered activity in atrial myocytes. *Am. J. Physiol. Heart Circ. Physiol.* **2008**, *294*, H2031–H2039. [[CrossRef](#)] [[PubMed](#)]
4. Sossalla, S.; Wagner, S.; Rasenack, E.C.; Ruff, H.; Weber, S.L.; Schondube, F.A.; Tirilomis, T.; Tenderich, G.; Hasenfuss, G.; Belardinelli, L.; et al. Ranolazine improves diastolic dysfunction in isolated myocardium from failing human hearts—role of late sodium current and intracellular ion accumulation. *J. Mol. Cell. Cardiol.* **2008**, *45*, 32–43. [[CrossRef](#)]
5. Maltsev, V.A.; Sabbah, H.N.; Higgins, R.S.; Silverman, N.; Lesch, M.; Undrovinas, A.I. Novel, ultraslow inactivating sodium current in human ventricular cardiomyocytes. *Circulation* **1998**, *98*, 2545–2552. [[CrossRef](#)]

6. Undrovinas, A.I.; Maltsev, V.A.; Sabbah, H.N. Repolarization abnormalities in cardiomyocytes of dogs with chronic heart failure: Role of sustained inward current. *Cell Mol. Life Sci.* **1999**, *55*, 494–505. [[CrossRef](#)]
7. Despa, S.; Islam, M.A.; Weber, C.R.; Pogwizd, S.M.; Bers, D.M. Intracellular Na(+) concentration is elevated in heart failure but Na/K pump function is unchanged. *Circulation* **2002**, *105*, 2543–2548. [[CrossRef](#)]
8. Toischer, K.; Hartmann, N.; Wagner, S.; Fischer, T.H.; Herting, J.; Danner, B.C.; Sag, C.M.; Hund, T.J.; Mohler, P.J.; Belardinelli, L.; et al. Role of late sodium current as a potential arrhythmogenic mechanism in the progression of pressure-induced heart disease. *J. Mol. Cell. Cardiol.* **2013**, *61*, 111–122. [[CrossRef](#)]
9. Djouhri, L.; Fang, X.; Okuse, K.; Wood, J.N.; Berry, C.M.; Lawson, S.N. The TTX-resistant sodium channel Nav1.8 (SNS/PN3): Expression and correlation with membrane properties in rat nociceptive primary afferent neurons. *J. Physiol.* **2003**, *550*, 739–752. [[CrossRef](#)]
10. Dib-Hajj, S.D.; Binshtok, A.M.; Cummins, T.R.; Jarvis, M.F.; Samad, T.; Zimmermann, K. Voltage-gated sodium channels in pain states: Role in pathophysiology and targets for treatment. *Brain Res. Rev.* **2009**, *60*, 65–83. [[CrossRef](#)]
11. Akopian, A.N.; Sivilotti, L.; Wood, J.N. A tetrodotoxin-resistant voltage-gated sodium channel expressed by sensory neurons. *Nature* **1996**, *379*, 257–262. [[CrossRef](#)]
12. Liu, M.; Wood, J.N. The roles of sodium channels in nociception: Implications for mechanisms of neuropathic pain. *Pain Med.* **2011**, *12* (Suppl. S3), S93–S99. [[CrossRef](#)]
13. Sotoodehnia, N.; Isaacs, A.; de Bakker, P.I.; Dorr, M.; Newton-Cheh, C.; Nolte, I.M.; van der Harst, P.; Muller, M.; Eijgelsheim, M.; Alonso, A.; et al. Common variants in 22 loci are associated with QRS duration and cardiac ventricular conduction. *Nat. Genet.* **2010**, *42*, 1068–1076. [[CrossRef](#)]
14. Chambers, J.C.; Zhao, J.; Terracciano, C.M.; Bezzina, C.R.; Zhang, W.; Kaba, R.; Navaratnarajah, M.; Lotlikar, A.; Sehmi, J.S.; Kooner, M.K.; et al. Genetic variation in SCN10A influences cardiac conduction. *Nat. Genet.* **2010**, *42*, 149–152. [[CrossRef](#)]
15. van den Boogaard, M.; Wong, L.Y.; Tessadori, F.; Bakker, M.L.; Dreizehnter, L.K.; Wakker, V.; Bezzina, C.R.; 't Hoen, P.A.; Bakkers, J.; Barnett, P.; et al. Genetic variation in T-box binding element functionally affects SCN5A/SCN10A enhancer. *J. Clin. Investig.* **2012**, *122*, 2519–2530. [[CrossRef](#)]
16. Ritchie, M.D.; Denny, J.C.; Zuvich, R.L.; Crawford, D.C.; Schildcrout, J.S.; Bastarache, L.; Ramirez, A.H.; Mosley, J.D.; Pulley, J.M.; Basford, M.A.; et al. Genome- and phenome-wide analyses of cardiac conduction identifies markers of arrhythmia risk. *Circulation* **2013**, *127*, 1377–1385. [[CrossRef](#)]
17. Bezzina, C.R.; Barc, J.; Mizusawa, Y.; Remme, C.A.; Gourraud, J.B.; Simonet, F.; Verkerk, A.O.; Schwartz, P.J.; Crotti, L.; Dagradi, F.; et al. Common variants at SCN5A-SCN10A and HEY2 are associated with Brugada syndrome, a rare disease with high risk of sudden cardiac death. *Nat. Genet.* **2013**, *45*, 1044–1049. [[CrossRef](#)]
18. Hu, D.; Barajas-Martinez, H.; Pfeiffer, R.; Dezi, F.; Pfeiffer, J.; Buch, T.; Betzenhauser, M.J.; Belardinelli, L.; Kahlig, K.M.; Rajamani, S.; et al. Mutations in SCN10A are responsible for a large fraction of cases of Brugada syndrome. *J. Am. Coll. Cardiol.* **2014**, *64*, 66–79. [[CrossRef](#)]
19. Pabel, S.; Ahmad, S.; Tirilomis, P.; Stehle, T.; Mustroph, J.; Knierim, M.; Dybkova, N.; Bengel, P.; Holzamer, A.; Hilker, M.; et al. Inhibition of NaV1.8 prevents atrial arrhythmogenesis in human and mice. *Basic Res. Cardiol.* **2020**, *115*, 20. [[CrossRef](#)]
20. Dybkova, N.; Ahmad, S.; Pabel, S.; Tirilomis, P.; Hartmann, N.; Fischer, T.H.; Bengel, P.; Tirilomis, T.; Ljubojevic, S.; Renner, A.; et al. Differential regulation of sodium channels as a novel proarrhythmic mechanism in the human failing heart. *Cardiovasc. Res.* **2018**, *114*, 1728–1737. [[CrossRef](#)]
21. Bengel, P.; Ahmad, S.; Tirilomis, P.; Trum, M.; Dybkova, N.; Wagner, S.; Maier, L.S.; Hasenfuss, G.; Sossalla, S. Contribution of the neuronal sodium channel Nav1.8 to sodium- and calcium-dependent cellular proarrhythmia. *J. Mol. Cell. Cardiol.* **2020**, *144*, 35–46. [[CrossRef](#)] [[PubMed](#)]
22. Bengel, P.; Dybkova, N.; Tirilomis, P.; Ahmad, S.; Hartmann, N.; Mohamed, B.A.; Krekeler, M.C.; Maurer, W.; Pabel, S.; Trum, M.; et al. Detrimental proarrhythmogenic interaction of Ca(2+)/calmodulin-dependent protein kinase II and Nav1.8 in heart failure. *Nat. Commun.* **2021**, *12*, 6586. [[CrossRef](#)] [[PubMed](#)]
23. Maurer, W.; Hartmann, N.; Argyriou, L.; Sossalla, S.; Streckfuss-Bomeke, K. Generation of homozygous Na(v)1.8 knock-out iPSC lines by CRISPR Cas9 genome editing to investigate a potential new antiarrhythmic strategy. *Stem Cell Res.* **2022**, *60*, 102677. [[CrossRef](#)] [[PubMed](#)]
24. Casini, S.; Marchal, G.A.; Kawasaki, M.; Nariswari, F.A.; Portero, V.; van den Berg, N.W.E.; Guan, K.; Driessen, A.H.G.; Veldkamp, M.W.; Mengarelli, I.; et al. Absence of Functional Nav1.8 Channels in Non-diseased Atrial and Ventricular Cardiomyocytes. *Cardiovasc. Drugs Ther.* **2019**, *33*, 649–660. [[CrossRef](#)] [[PubMed](#)]
25. Hindricks, G.; Potpara, T.; Dagres, N.; Arbelo, E.; Bax, J.J.; Blomstrom-Lundqvist, C.; Boriani, G.; Castella, M.; Dan, G.A.; Dilaveris, P.E.; et al. 2020 ESC Guidelines for the diagnosis and management of atrial fibrillation developed in collaboration with the European Association for Cardio-Thoracic Surgery (EACTS): The Task Force for the diagnosis and management of atrial fibrillation of the European Society of Cardiology (ESC) Developed with the special contribution of the European Heart Rhythm Association (EHRA) of the ESC. *Eur. Heart J.* **2021**, *42*, 373–498. [[CrossRef](#)]
26. Reiffel, J.A.; Camm, A.J.; Belardinelli, L.; Zeng, D.; Karwatowska-Prokopczuk, E.; Olmsted, A.; Zareba, W.; Rosero, S.; Kowey, P. The HARMONY Trial: Combined Ranolazine and Dronedarone in the Management of Paroxysmal Atrial Fibrillation: Mechanistic and Therapeutic Synergism. *Circ. Arrhythmia Electrophysiol.* **2015**, *8*, 1048–1056. [[CrossRef](#)]

27. Sossalla, S.; Kallmeyer, B.; Wagner, S.; Mazur, M.; Maurer, U.; Toischer, K.; Schmitto, J.D.; Seipelt, R.; Schondube, F.A.; Hasenfuss, G.; et al. Altered Na(+) currents in atrial fibrillation effects of ranolazine on arrhythmias and contractility in human atrial myocardium. *J. Am. Coll. Cardiol.* **2010**, *55*, 2330–2342. [[CrossRef](#)]
28. Fischer, T.H.; Herting, J.; Mason, F.E.; Hartmann, N.; Watanabe, S.; Nikolaev, V.O.; Sprenger, J.U.; Fan, P.; Yao, L.; Popov, A.F.; et al. Late INa increases diastolic SR-Ca²⁺-leak in atrial myocardium by activating PKA and CaMKII. *Cardiovasc. Res.* **2015**, *107*, 184–196. [[CrossRef](#)]
29. Hartmann, N.; Mason, F.E.; Braun, I.; Pabel, S.; Voigt, N.; Schotola, H.; Fischer, T.H.; Dobrev, D.; Danner, B.C.; Renner, A.; et al. The combined effects of ranolazine and dronedarone on human atrial and ventricular electrophysiology. *J. Mol. Cell. Cardiol.* **2016**, *94*, 95–106. [[CrossRef](#)]
30. White, C.M.; Nguyen, E. Novel Use of Ranolazine as an Antiarrhythmic Agent in Atrial Fibrillation. *Ann. Pharmacother.* **2017**, *51*, 245–252. [[CrossRef](#)]
31. Ahmad, S.; Tirilomis, P.; Pabel, S.; Dybkova, N.; Hartmann, N.; Molina, C.E.; Tirilomis, T.; Kutschka, I.; Frey, N.; Maier, L.S.; et al. The functional consequences of sodium channel Na(V) 1.8 in human left ventricular hypertrophy. *ESC Heart Fail.* **2019**, *6*, 154–163. [[CrossRef](#)]
32. Jabbari, J.; Olesen, M.S.; Yuan, L.; Nielsen, J.B.; Liang, B.; Macri, V.; Christophersen, I.E.; Nielsen, N.; Sajadieh, A.; Ellinor, P.T.; et al. Common and rare variants in SCN10A modulate the risk of atrial fibrillation. *Circ. Cardiovasc. Genet.* **2015**, *8*, 64–73. [[CrossRef](#)]
33. Maier, L.S.; Sossalla, S. The late Na current as a therapeutic target: Where are we? *J. Mol. Cell. Cardiol.* **2013**, *61*, 44–50. [[CrossRef](#)]
34. Pfeufer, A.; van Noord, C.; Marcianti, K.D.; Arking, D.E.; Larson, M.G.; Smith, A.V.; Tarasov, K.V.; Muller, M.; Sotoodehnia, N.; Sinner, M.F.; et al. Genome-wide association study of PR interval. *Nat. Genet.* **2010**, *42*, 153–159. [[CrossRef](#)]
35. Dybkova, N.; Wagner, S.; Backs, J.; Hund, T.J.; Mohler, P.J.; Sowa, T.; Nikolaev, V.O.; Maier, L.S. Tubulin polymerization disrupts cardiac beta-adrenergic regulation of late INa. *Cardiovasc. Res.* **2014**, *103*, 168–177. [[CrossRef](#)]
36. Yang, T.; Atack, T.C.; Stroud, D.M.; Zhang, W.; Hall, L.; Roden, D.M. Blocking Scn10a channels in heart reduces late sodium current and is antiarrhythmic. *Circ. Res.* **2012**, *111*, 322–332. [[CrossRef](#)]
37. Savio-Galimberti, E.; Weeke, P.; Muhammad, R.; Blair, M.; Ansari, S.; Short, L.; Atack, T.C.; Kor, K.; Vanoye, C.G.; Olesen, M.S.; et al. SCN10A/Nav1.8 modulation of peak and late sodium currents in patients with early onset atrial fibrillation. *Cardiovasc. Res.* **2014**, *104*, 355–363. [[CrossRef](#)]
38. Kleinsorge, M.; Cyganek, L. Subtype-Directed Differentiation of Human iPSCs into Atrial and Ventricular Cardiomyocytes. *STAR Protoc.* **2020**, *1*, 100026. [[CrossRef](#)]

Disclaimer/Publisher’s Note: The statements, opinions and data contained in all publications are solely those of the individual author(s) and contributor(s) and not of MDPI and/or the editor(s). MDPI and/or the editor(s) disclaim responsibility for any injury to people or property resulting from any ideas, methods, instructions or products referred to in the content.